Research Reports Biomaterials & Bioengineering: Electron Microscopy, Micro-analysis, and X-ray Diffraction Characterization of the Mineral-like Tissue Deposited by Human Cementum Tumor-derived Cells

H. Arzate, M.A. Alvarez-Perez, O. Alvarez-Fregoso, A. Wusterhaus-Chávez, J. Reyes-Gasga and L.A. Ximenez-Fyvie

J DENT RES 2000; 79; 28
DOI: 10.1177/00220345000790010301

RESEARCH REPORTS
Biomaterials & Bioengineering

H. Arzate[1]*, M.A. Alvarez-Pérez[2], O. Alvarez-Fregoso[3], A. Wusterhaus-Chávez[4], J. Reyes-Gasga[5], and L.A. Ximénez-Fyvie[1]

[1]Laboratorio de Biología Celular y Molecular, División de Estudios de Posgrado e Investigación, Facultad de Odontología, UNAM, Cd. Universitaria, 04510 México DF; [2]Instituto de Fisiología Celular, UNAM, México; [3]Instituto de Investigación en Materiales, UNAM, México; [4]CMN "20 de Noviembre", ISSSTE, México; and [5]Instituto de Física, UNAM, México; *corresponding author, harzate@servidor.unam.mx

J Dent Res 79(1): 28-34, 2000

Electron Microscopy, Micro-analysis, and X-ray Diffraction Characterization of the Mineral-like Tissue Deposited by Human Cementum Tumor-derived Cells

ABSTRACT

The nature and characteristics of the mineralized-like tissue deposited by cementoblasts are not well-known due to the difficulties in obtaining and culturing cells representing the cementum phenotype. We hypothesized that a putative cementoblastic cell line derived from a human cementoblastoma could serve as a suitable model to study the physical, chemical, and morphological features of the cementum-like tissue deposited *in vitro*. The cementoblastoma cell line was studied by transmission electron, high resolution, scanning, and atomic force microscopy and compared with human cellular cementum, human osteoblasts, and human alveolar bone. The analyses of the crystals and mineral-like tissue in the cell line were performed by x-ray diffraction microscopy and energy-dispersive x-ray micro-analysis. TEM examination of cementoblastoma cells revealed the presence of electron-dense intracellular vesicles surrounded by a membrane that contained filaments and needle-like structures. The diffraction patterns obtained from the intracellular material and human cellular cementum were similar, with D-spacings of 3.36 and 2.8, consistent with those of hydroxyapatite (3.440 and 2.814). The composition of the mineral-like tissue had a Ca/P ratio of 1.60 for cementoblastoma cells and 1.97 for human cellular cementum. Na (5.29%) and Cl (1.47%) were present in the composition of cementoblastoma cells. Human cellular cementum additionally contained Mg (4.95%). Osteoblastic cells showed a Ca/P ratio of 1.6280. Na represented 4.52% and Cl 1.22% of its composition. Human alveolar bone had a Ca/P ratio value of 2.01. Na (6.63%), Mg (2.10%), and Cl (0.84%) were also present. All samples examined represented biological-type hydroxyapatite. Based on the compositional and morphological features, these findings indicate that cementoblastoma-derived cells express the human cellular cementum phenotype.

KEY WORDS: cementoblast, osteoblast, mineralization, hydroxyapatite, and cell culture.

Received November 12, 1998; Last Revision June 3, 1999; Accepted June 4, 1999

INTRODUCTION

Cementoblasts are believed to be derived from multipotential stem cells in the endosteal spaces of the paravascular vessels of the alveolar bone (McCulloch *et al.*, 1987). These stem cells have the capacity of self-renewal and, under the influence of unknown factors, are thought to give rise to progenitors of each cell type that comprise the periodontium, such as osteoblasts, cementoblasts, and periodontal ligament fibroblasts (Gould *et al.*, 1977). Cementoblast progenitor cells have been found in the paravascular zones in the adult periodontal ligament of mice (McCulloch *et al.*, 1983; Melcher *et al.*, 1987), although mice do not constitute a parallel model for the study of cementogenesis in humans (Bosshardt and Schroeder, 1996).

Cells representing the cementum phenotype have not been isolated and propagated in culture, due in part to the lack of a cementum biological marker and in part to the technical difficulties in obtaining a pure population of cementoblasts. The conditions necessary to isolate cementoblasts have not yet been established, although several attempts have been made to obtain a population of cementoblasts and culture them *in vitro* (Arzate *et al.*, 1992a; D'Errico *et al.*, 1997; Grzesik *et al.*, 1998; MacNeil *et al.*, 1998). We recently proposed an alternative approach to obtain cells that express the cementoblast phenotype. Cells from a human cementoblastoma were isolated. This cell line may represent a cloned cell population of human cementoblasts. Preliminary *in vitro* studies have shown that these cells expressed several markers associated with mineral tissue formation, such as alkaline phosphatase (AlP) and osteopontin (OPN). Importantly, the cementoblastoma-derived cells expressed cementum attachment protein (CAP), which is restricted to cementum (Arzate *et al.*, 1992b). The preliminary data showed that cementoblastoma-derived cells deposited mineral-like tissue *in vitro* and had characteristics different from those of human alveolar bone cells *in vitro* (Arzate *et al.*, 1998).

Since very little is known about the nature of the mineralized-like tissue produced by cultured putative cementoblasts, this present work was designed to study the ultrastructural characteristics of cementoblastoma-derived cells and to investigate both the characteristics and the nature of the mineral-like tissue formed by these cells. The findings were compared with those of human cellular cementum, human osteoblastic-derived cells, and human alveolar bone. The characterization and analysis were performed by transmission electron microscopy (TEM), high-resolution transmission electron microscopy (HRTEM), scanning electron microscopy (SEM), atomic force microscopy (AFM), energy-dispersive x-ray micro-analysis (EDX), and x-ray diffraction microscopy (XRD).

MATERIALS & METHODS

Cell Culture

Human cementoblastoma and alveolar bone specimens were obtained according to the protocols approved by the Internal Review Board of the School of Dentistry, National Autonomous University of México. Human alveolar bone and

cementoblastoma-derived cells were obtained from a 38-year-old male patient with a mandibular cementoblastoma. The osteoblastic and cementoblastoma-derived cells were cultured by the explant technique described elsewhere (Narayanan and Page, 1976). Cells were cultured in Dulbecco's modified Eagle's medium (DMEM) (Sigma Chem. Co., St. Louis, MO, USA) supplemented with 10% fetal bovine serum (FBS) and antibiotic solution (penicillin 100 U/mL, streptomycin 100 μg/mL). Confluent monolayers of cells were passaged by trypsinization (Trypsin-EDTA, Gibco Laboratories, Grand Island, NY, USA), washed with full medium, and recultured in 75-cm^2 tissue culture flasks in a humidified incubator at 37°C in an atmosphere of 5% CO_2 and air. Cells at the 2nd passage were used for all experimental procedures.

Atomic Force Microscopy (AFM)

AFM was used to determine the morphology and homogeneity of the mineral-like tissue deposited by cementoblastoma-derived and osteoblastic cells. AFM (Park Scientific Instruments, Santa Barbara, CA, USA) was used with an AutoProbe in contact and constant mode (5 nanometers). Cementum tumor and osteoblastic cells were plated at 2 x 10^4 in 24-well culture plates (Costar Corporation, Cambridge, MA, USA) onto a silicon (1,1,1) monocrystal substrate and cultured for 14 days in DMEM supplemented with 10% FBS, antibiotics, 50 μg/mL ascorbic acid, 10 mM of β-glycerophosphate, and 10^{-7} M dexamethasone. We monitored the cultures at 3, 7, and 11 days to detect calcium salt precipitation in the cultures by using Alizarin red S staining at pH 4.1. The medium was changed every other day. After 14 days of incubation, osteoblastic and cementoblastoma-derived cells were rinsed three times with ice-cold phosphate-buffered saline (PBS); culture plates were fixed *in situ* by the addition of 70% ethyl alcohol and air-dried. To reveal similarities between the human cementum tumor cell cultures and human cementum, we processed a piece of 3-mm^2 of human cellular cementum as described above for examination with AFM. A piece of human alveolar bone (3 mm^2) was also examined with AFM to show differences with human cementum and cementoblastoma-derived cells.

Energy-dispersive X-ray Micro-analysis (EDX)

The composition of the mineral-like tissue formed by the cementoblastoma-derived and osteoblastic cells was analyzed. Cells were plated onto a silicon (1,1,1) monocrystal substrate at initial density 2 x 10^4 in 24-well plates and cultured for 14 days in DMEM supplemented with 10% FBS, antibiotics, 50 μg/mL ascorbic acid, 10 mM of β-glycerophosphate, and 10^{-7} M dexamethasone. The cultures were analyzed by means of a Leica-Cambridge 440 scanning electron microscope fitted with a Pentafet energy-dispersive x-ray micro-analysis microprobe. After the cultures were terminated, they were washed with PBS, fixed in 70% ethyl alcohol, and air-dried. The surfaces of the cultures as well as the human cellular cementum and human alveolar bone were covered with a thin gold film about 100 nm thick, to avoid electron disturbances that could affect micro-analysis and SEM images. All analyses were carried out at 20 kV for 300 sec (Cuisinier *et al.*, 1991; Van Dijk *et al.*, 1995).

Transmission Electron Microscopy (TEM)

Cementoblastoma-derived cells were plated at 2 x 10^4 initial density in DMEM supplemented as described above in 24-well culture plates. The medium was replaced with fresh medium every other day, and cultures were kept under these conditions for 14 days. They were then briefly washed with PBS and fixed first *in situ* by the addition of 2.5% glutaraldehyde (buffered at pH 7.4 with 0.1 M sodium cacodylate) at 4°C for 30 min. Second, the cells were fixed with 1% OsO_4 in the same buffer at 4°C for 1 hr. The samples were then dehydrated briefly in ascending concentrations of ethyl alcohol, followed by propylene oxide as a clearing agent. Cultures were embedded in epoxy resin. Semithin sections about 2 μm thick were obtained and stained with toluidine blue for light microscopy orientation. Ultra-thin sections (about 80 to 90 nm thick) cut with a diamond knife (Diatome, Biel, Switzerland) were mounted on Formvar-coated 150-mesh copper grids and examined with and without uranyl acetate and lead citrate (U-Pb) staining. Examination and recording were performed with a Phillips 201 and a Jeol 100 CX fitted with an SEM unity (STEM). A JEOL 400EX transmission electron microscope was used for the high-resolution analysis of the cultures.

Selected Area Diffraction Patterns by TEM

To reveal the formed mineral phase, we used selected areas of ultra-thin and unstained sections, mounted as described above, for electron diffraction and nanodiffraction techniques. D-spacings of diffraction patterns were calibrated against those of the gold standard obtained with identical diffraction conditions. The mineral phase was analyzed by means of a JEOL 100 CX analytical transmission microscope. All analyses were performed at 100 kV.

RESULTS

Transmission Electron Microscopy (TEM)

Light microscopy monitoring, together with Alizarin red S staining, showed that cementoblastoma-derived cells had formed the first mineralized structures (nodules) after 4 to 7 days in culture. The TEM examination revealed that cementoblastoma-derived cells contained all the cytoplasmic organelles characteristic of protein synthesis and secretion. Arrays of rough endoplasmic reticulum were disposed around the nuclear membrane. Golgi complex was observed in perinuclear areas. Primary lysosomes and mitochondria predominated in various cytoplasmic areas (Fig. 1). Membrane-bound vesicular structures were found intracellularly (Fig. 2). The vesicles had round to oval shapes, with diameters of 50 to 100 nm. The vesicles were electron-dense. Filament and needle-like crystals were observed in the vesicles (Fig. 2 inset). Examination of these nanocrystals at higher resolution with TEM showed both homogeneous and heterogeneous spatial crystal arrangements (Fig. 3).

Electron Diffraction and EDX Micro-analysis

Selected area diffraction patterns from unstained sections of the cementoblastoma-derived cells were obtained for the analysis of mineral deposits at 14 days of culture. Because of the nanosize of the formed crystals, they revealed patterns of concentric double rings. The inner double rings represent D-spacing (3.36 and 2.8, respectively) values consistent with those of hydroxyapatite (3.440 and 2.814) (Fig. 4). These D-spacings are in agreement with those registered from the HRTEM images as shown in Fig. 3.

X-ray EDX Micro-analysis

The Ca/P ratio and composition of the mineral-like tissue deposited by cementoblastoma-derived cells revealed prominent energy peaks for calcium and phosphorus similar to those for biological apatite (Fang *et al.*, 1994).

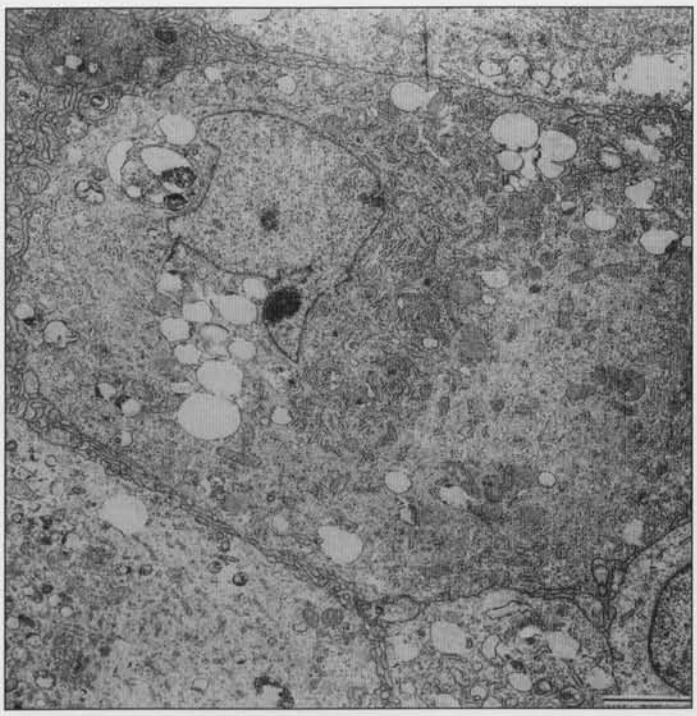

Figure 1. Electron micrograph of a cementoblastoma-derived cell having a nucleus with diffused heterochromatin and cytoplasm with rough endoplasmic reticulum, various amounts of mitochondria, and Golgi complex. 12,230X. Bar = 2.5 μm.

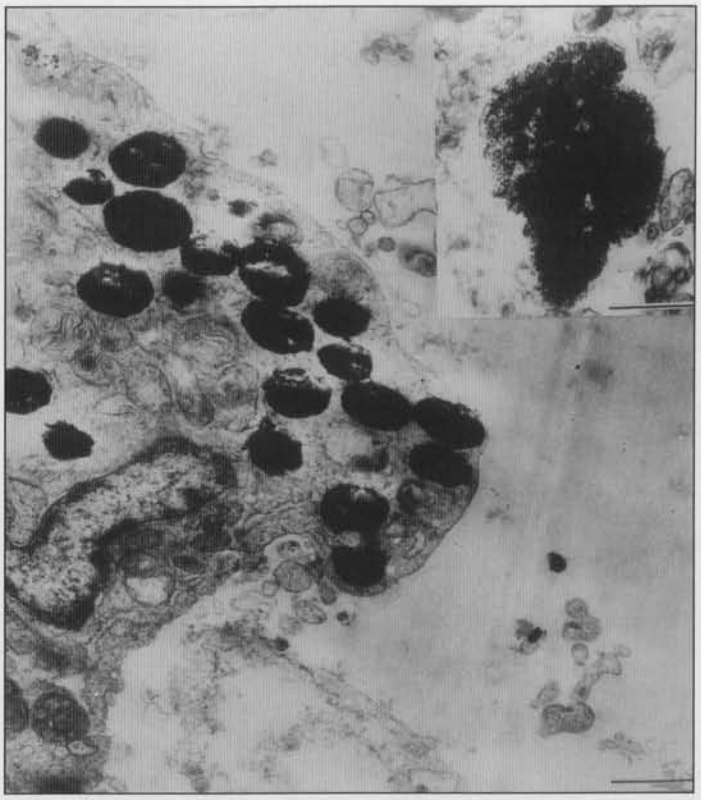

Figure 2. Electron micrograph of cementoblastoma-derived cells shows intracytoplasmic electron-dense granules with a rough shape. 14,000X. Bar = 1.0 μm. Intracellular vesicle surrounded by a membrane. Note filament and needle-like structures inside the vesicle (inset). 30,000X. Bar = 0.3 μm.

Cementoblastoma-derived cells had 36.64 and 22.48 atomic percentages of Ca and P, respectively. Other elements such as Na (5.29%) and Cl (1.47%) were present in its global composition. Human cellular cementum revealed Mg 4.95, Na 8.43, Cl 2.92, P 28.18, and Ca 55.52 atomic percentages in its composition. The Ca/P ratio values (1.6056 for cementum cells and 1.9700 for human cellular cementum) correspond well with the biological hydroxyapatite value as determined by EDX. Osteoblastic cells showed 34.2 and 21.3 atomic percentages of Ca and P, respectively, with a Ca/P ratio of 1.6280. Na represented 4.52 and Cl 1.22 atomic percentage. Human alveolar bone had Na 6.63, Mg 2.10, Cl 0.84, P 35.33, and Ca 55.11 atomic percentage in its composition. Human alveolar bone had a Ca/P ratio value of 2.01. Both osteoblastic cells and alveolar bone values correspond to those of biological-type hydroxyapatite as determined by EDX (Figs. 5A, 5B).

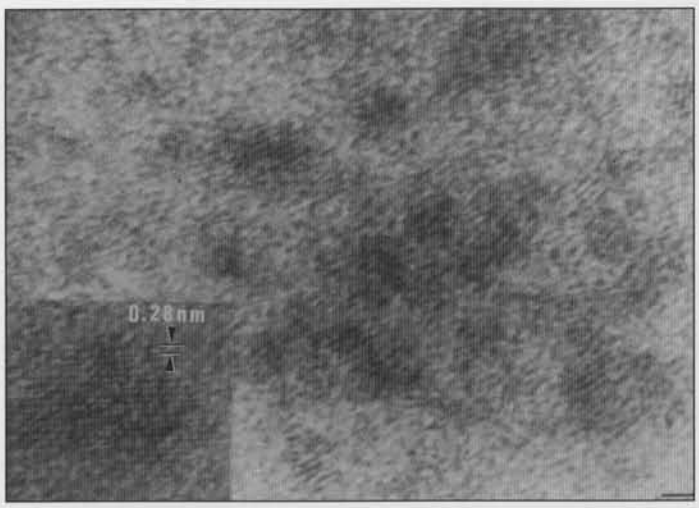

Figure 3. High-resolution transmission electron microscopy (HRTEM). A representative image from cementum cells showing a heterogeneous and homogeneous (inset) arrangement of hydroxyapatite crystal. Bar = 50 nm.

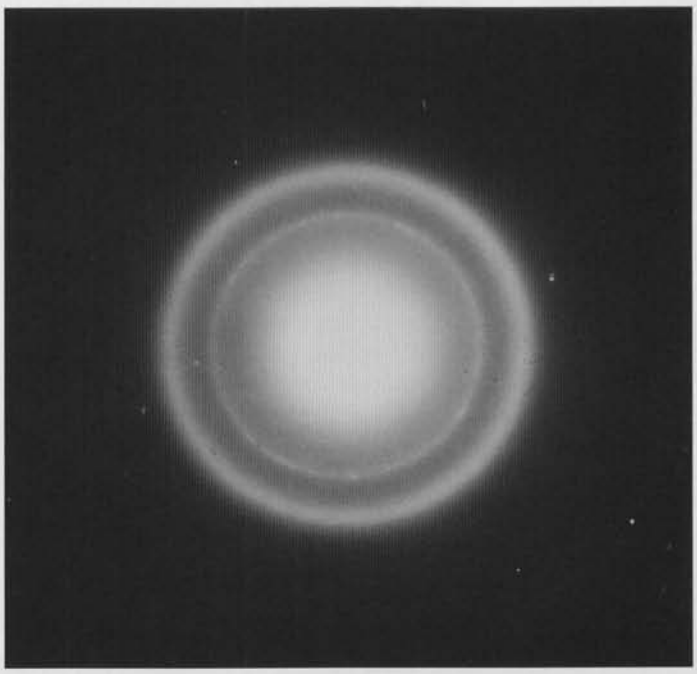

Figure 4. Electron diffraction pattern from mineralized intracellular vesicles observed in cementoblastoma-derived cells.

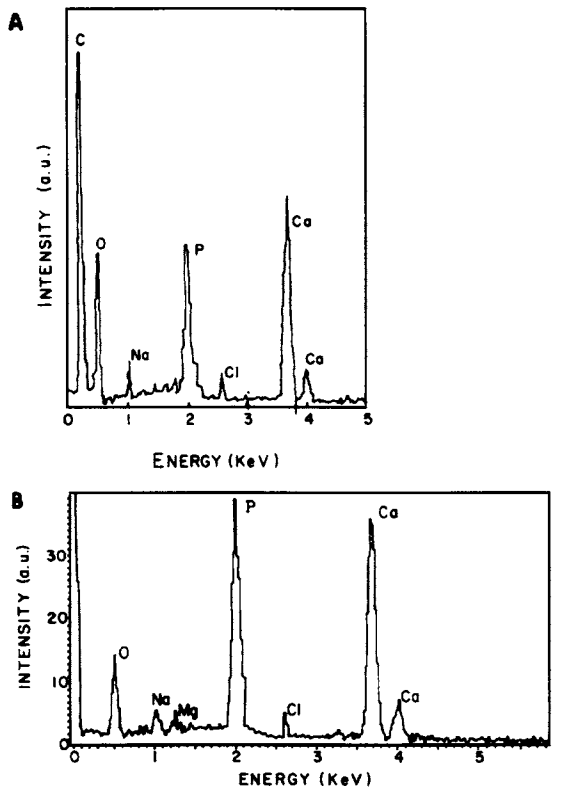

Figure 5. (A) Representative energy-dispersive x-ray micro-analysis spectrum of mineralized areas of cementoblastoma-derived and osteoblastic cells cultured on a silicon (1,1,1) substrate, showing prominent peaks of calcium (Ca), phosphorus (P), and peaks representing sodium (Na) and chloride (Cl). (B) Human cellular cementum and human alveolar bone additionally presented a peak of magnesium (Mg) in its global composition.

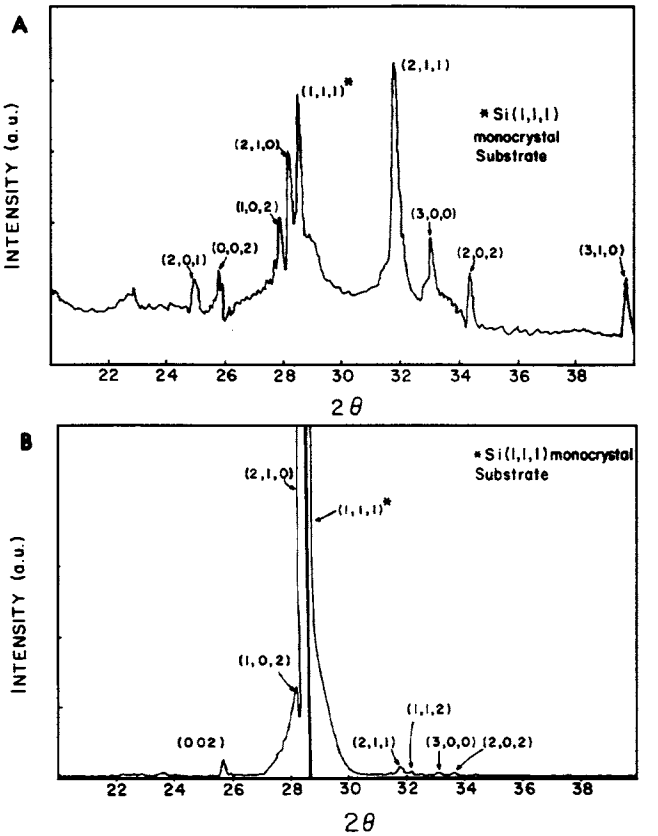

Figure 6. A representative analysis of the crystallinity by means of the x-ray diffraction technique from mineralized areas of cementoblastoma-derived cells and human cellular cementum, showing the XRD pattern with broad peaks, indicating (A) heterogeneous grain size and (B) a better crystallinity with (2,1,0) preferential orientation and homogeneous crystallites.

X-ray Diffraction Analysis

The crystallinity of the mineralization process was evaluated by x-ray diffraction. The mineral deposited by cementoblastoma-derived cells showed crystallinity with both non-homogeneous (2,1,1, 2,1,0, 2,0,1, etc.) and preferential orientation (2,1,0) of hydroxyapatite crystallites. The heterogeneous diffraction pattern obtained from both cementoblastoma-derived cells and human cellular cementum showed a differential organization of the mineral phase (Fig. 6A). The well-defined diffraction peak obtained from the cementoblastoma-derived cells and human cellular cementum resembles a textured preferentially oriented and homogenized layer of mineral (Fig. 6B). Both patterns were indexed with the hydroxyapatite standard patterns of the JCPDS (Joint Committee on Powder Diffraction Standards No. 9-432 file for calcium hydroxyapatite) (JCPDS, 1998).

Atomic Force Microscopy

The morphology of the mineral deposited by cementoblastoma-derived cells cultured onto a silicon (1,1,1) monocrystal substrate revealed small granular particles (1 ± 0.5 μm) and highly crystalline plaques with needle-like morphology (35 ± 15 μm) for both cementoblastoma-derived cells and human cellular cementum. Cementum cell cultures and human cellular cementum showed a layered structure demarcated by incremental cell lines (Figs. 7A, 7B, respectively). The crystal morphology revealed the submicron size (0.2 μm) of the granular spherical particles that form the agglomerates (Fig. 8A). The frontal needle-like crystals had a grain submicron size average about 0.5 ± 0.3 μm (Fig. 8B). Human cellular cementum revealed similar hydroxyapatite crystal morphology. They showed agglomerates with a granular disposition that resembled that of the cementum tumor cell cultures. The microsize of the granules observed in human cellular cementum was heterogeneous to a size range between 0.2 μm and 0.002 μm (Figs. 8C, 8D). Osteoblastic cells showed needle-like crystals oriented perpendicular to the silicon (1,1,1) monocrystal substrate and organized in plaque-like structures with a size range of 2.2 ± 0.3 μm. Human alveolar bone had well-oriented longitudinal crystals with a size range between 2.0 and 4.0 μm, and with a lamellar pattern. (Figs. 8E, 8F, respectively). The examination of the cementoblastoma-derived cell cultures with SEM revealed mineralized areas which were formed by agglomerates of homogeneous size with spherical and ring-like shapes (Fig. 9A). Human cellular cementum showed similar agglomerates of heterogeneous size and morphology (Fig. 9B).

DISCUSSION

Human cementoblastoma-derived cells showed membrane-bound intracellular vesicular structures after 14 days in culture. The vesicles showed heavy electron-dense mineralized material that contained filaments and needle-like crystals. The function of these vesicles is still obscure. However, it is possible that they

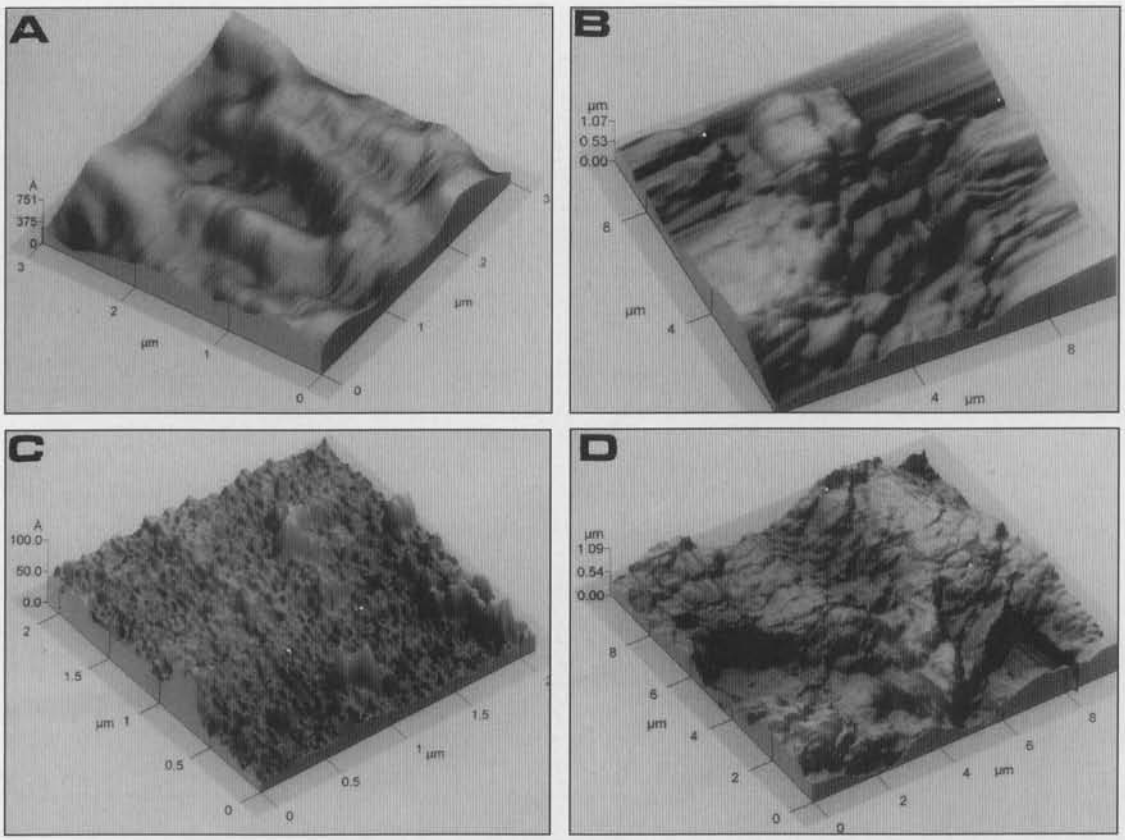

Figure 7. (A) AFM three-dimensional images showed lamellar arrangement of the mineral-like tissue formed by cementoblastoma-derived cells. (B) Human cellular cementum showing similar spatial disposition of the mineral agglomerates and also parallel alignment of the mineral plaques. (C) Osteoblastic cells showed longitudinal needle-like arrangement of the apatite crystals. (D) Human alveolar bone showing apatite crystals oriented similar to those observed in osteoblastic cell cultures.

represent Ca/P storing mitochondria (Lehninger, 1970; Matthews *et al.*, 1970; Brighton and Hunt, 1976; Appleton and Morris, 1979; Landis *et al.*, 1980; Wuthier, 1982). This concept is supported, since the calcium complex is located predominantly in mitochondria as well as in cell membranes, and represents the initial mineralization site. It also suggests that intracellular calcium plays a significant role in matrix calcification (Sasagawa, 1988). It is possible that, during cementogenesis, cementoblasts liberate Ca/P storing vesicles by physiological cell death to increase the amount of mineral constituents at sites of mineralization, and that those crystals could serve as initial extracellular nucleation centers for hydroxyapatite crystals (Zimmermann *et al.*, 1991; Zimmermann, 1994). Although the importance of cell necrosis in the process of mineralization is as yet unclear, it is important to note that a secretion process from these vesicles was not observed. As shown in the AFM images, the mineral accumulation had morphological processes ranging from amorphous-globular to crystalline filaments and needle-like morphology. From these results, we assume that this transformation phase takes place within intracellular vesicular structures. This finding provides additional evidence that initial mineralization requires a micro-environment limited by a membrane (vesicular) structure derived from the cells. This is not a unique finding, since intracellular vesicles have been observed in osteoblasts

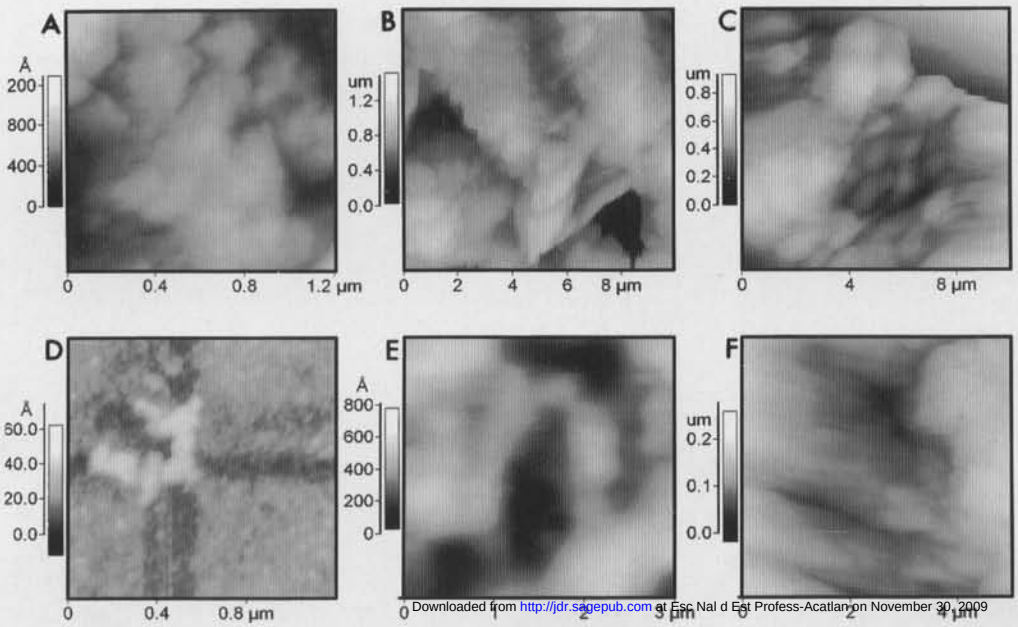

Figure 8. The morphologic features obtained by atomic force microscopy showed that the cementoblastoma cells and human cellular cementum mineral deposits were composed of large agglomerates of tiny submicron-size granular particles (A and D, respectively). Other mineralized areas showed large plaques with some needle-like and small granular particles (B and C, for cementoblastoma-derived cells and human cellular cementum, respectively). (E) Osteoblastic cells showed needle-like crystals oriented perpendicular to the silicon (1,1,1) monocrystal substrate and organized in plaque-like structures with micron size particles. (F) Human alveolar bone had well-oriented longitudinal crystals with a micron size range and with a filament-like pattern.

and associated with transitional stages between mitochondria and intracellular vesicles surrounded by double membranes (Volpe *et al.*, 1988). The occurrence of intracellular vesicles has also been observed in odontoblasts and associated with the mineralization process (Hayashi *et al.*, 1993). AFM images and x-ray EDX micro-analysis demonstrated that cementoblastoma-derived cells and human cellular cementum had compositional and morphological features in common. Both showed similar composition and Ca/P ratios. Importantly, the cementoblastoma-derived cells produced biological-type apatite. The morphological features observed in the cementoblastoma cultures resembled those of human cellular cementum. Crystals and a layered structure demarcated by incremental lines were also evident. This lamellar pattern is characteristic of human cellular cementum (Yamamoto *et al.*, 1998). Osteoblastic cells and human alveolar bone showed needle-like crystals with longitudinal arrangement of the mineral-like tissue. However, the morphological features observed in human osteoblastic cells and human alveolar bone were clearly different from those observed in human cementoblastoma-derived cells and human cellular cementum. An important finding in the osteoblastic cells and cementoblastoma-derived cultures was that they do not have Mg in their global composition. We could thus assume that magnesium could interact in the formation, stability, and maturation of biological hydroxyapatite and related Ca/P ratio. This could explain the lower Ca/P ratio values obtained from the cultures when compared with those obtained from human cellular cementum and alveolar bone (LeGeros and Kojkowska, 1989).

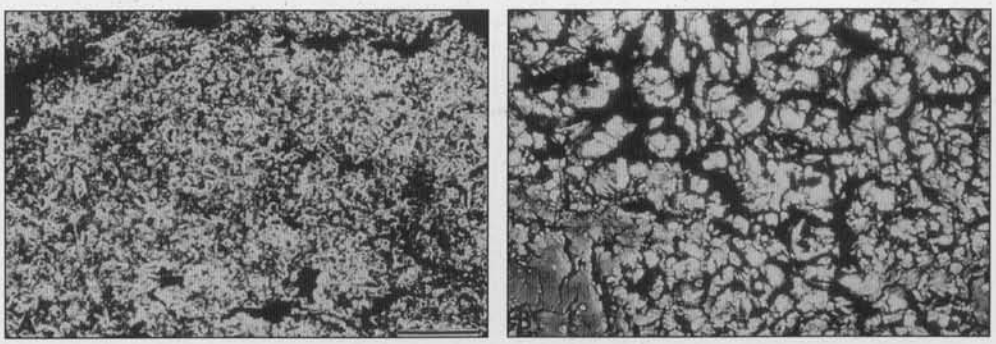

Figure 9. Mineralized features observed by SEM in (A) cementoblastoma-derived cells and (B) human cellular cementum, showing spherical and ring-like shapes. Bar = 100 μm (A) and 10 μm (B).

It has previously been demonstrated that globular-like structures, which represent initial nucleation centers of hydroxyapatite crystals, are localized intracellularly (Arzate *et al.*, 1998). XRD images showed both a heterogeneous and homogeneous preferential orientation of hydroxyapatite crystals. A similar spatial arrangement of hydroxyapatite crystals was observed in human cellular cementum. The organic structure of the mineral-like tissue formed by the cementoblastoma-derived cells was shown to be granular and needle-like. These features matched those demonstrated in human cellular cementum (Bonucci, 1971, 1987; Goldberg *et al.*, 1980; Bishop and Warshawsky, 1982; Hayashi *et al.*, 1986; Hayashi, 1985, 1989). The composition, morphological appearance of the mineral-like tissue, and size and shape of the hydroxyapatite crystals formed by cementoblastoma-derived cells, when compared with those of human cellular cementum, strongly support the contention that the mineral-like tissue formed by the cementoblastoma-derived cells is human cellular cementum, produced *in vitro*. In the culture system reported here and in our culture conditions, cementoblastoma-derived and osteoblastic cells were able to grow and differentiate when they were plated onto a silicon monocrystal substrate. In addition, they were able to produce biological-type hydroxyapatite. However, when plastic substrate was used, there was an absence of Na and Cl in the global composition of the mineral-like tissue deposited by the cells. This suggests that the substrate influenced the secretory properties of the cells to produce biological-type hydroxyapatite. This culture system, then, could be useful to study how the inductors-precursors of the mineralization process influence the morphology and composition of mineralized-like tissue. The electron diffraction patterns of the intracellular mineral deposits showed concentric inner rings and D-spacings identical to those of hydroxyapatite. These results clearly showed that the crystals formed in this system represent combined organic-inorganic structures, which contain a solid phase deposit, which is a biological-type apatite. The combined data from chemical, x-ray diffraction, TEM, HRTM, electron diffraction, and SEM analyses have allowed for the precise identification of the crystalline components of the cementum-like tissue deposited by the putative cementoblasts and from human cellular cementum.

We have further characterized the ultrastructural features, nature, and physical structure of the mineral deposited by cementoblastoma-derived cells, which appear to be almost identical to those characteristics of cellular cementum. Although cementum and alveolar bone cells share a common stem cell, from the morphological and compositional differences between cementoblastoma-derived and osteoblastic cells and from their similarities to human cellular cementum, our results lead us to conclude that the cementoblastoma-derived cells expressed the cellular cementum phenotype. Differences between present results and those from other mineralizing cells may indicate molecular variations in the mineralization pathways. A new approach to the analysis of the three-dimensional structure, the composition of the mineral-matrix complex, and the arrangement of the apatite crystallites during the cementogenesis process *in vitro* is proposed.

ACKNOWLEDGMENTS

The authors are indebted to R. Fragoso, M.A. Leyva, P. Mexía, R. Hernández, G. Mondragón, C. Angeles, L. Baños, and A. Caballero from CINVESTAV-México, IF-UNAM, ININ-México, and IIM-UNAM for their assistance during the course of this study. Their support is appreciated. This work was supported by DGAPA-UNAM Grant IN200597 and CONACYT Grant 0057P-M to H.A.

REFERENCES

Appleton J, Morris DC (1979). The use of the potassium pyroantimonate-osmium method as a means of identifying and localizing calcium at the ultrastructural level in the cells of calcifying systems. *J Histochem Cytochem* 27:676-680.

Arzate H, Olson SW, Page RC, Narayanan AS (1992a). Isolation of human tumor cells that produce cementum proteins in culture. *Bone Miner* 18:15-30.

Arzate H, Olson SW, Page RC, Gown AM, Narayanan AS (1992b). Production of a monoclonal antibody to an attachment protein derived from human cementum. *FASEB J* 6:2990-2995.

Arzate H, Alvarez-Pérez MA, Aguilar-Mendoza ME, Alvarez-Fregoso O (1998). Human cementum tumor cells have different features from human osteoblastic cells *in vitro*. *J Periodont Res* 33:249-258.

Bishop MA, Warshawsky H (1982). Electron microscopic studies on the potential loss of crystallites from routinely processed sections of young enamel in the rat incisor. *Anat Rec* 202:177-186.

Bonucci E (1971). The locus of initial calcification in cartilage and bone. *Clin Orthop* 78:108-139.

Bonucci E (1987). Is there a calcification factor common to all calcifying matrices? *Scanning Microsc* 1:1089-1102.

Bosshardt DD, Schroeder HE (1996). Cementogenesis reviewed: a comparison between human premolars and rodent molars. *Anat Rec* 245:267-292.

Brighton CT, Hunt RM (1976). Histochemical localization of calcium in growth plate mitochondria and matrix vesicles. *Fed Proc* 35:143-147.

Cuisinier FJ, Glaisher RW, Voegel JC, Hutchison JL, Bres EF, Frank RM (1991). Compositional variations in apatites with respect to preferential ionic extraction. *Ultramicroscopy* 36:297-305.

D'Errico JA, MacNeil RL, Takata T, Berry J, Strayhorn C, Somerman MJ (1997). Expression of bone associated markers by tooth root lining cells, in situ and *in vitro*. *Bone* 20:117-126.

Fang Y, Agrawal DK, Roy DM (1994). Thermal stability of synthetic hydroxyapatite. In: Handbook of bioactive ceramics. Vol. III. Boca Raton, FL: CRC Press, pp. 269-282.

Goldberg M, Molon Noblot M, Septier D (1980). Effects of 2 methods of demineralization on the preservation of glycoproteins and proteoglycans in the intertubular and peritubular dentin in the horse [in French]. *J Biol Buccale* 8:315-330.

Gould TR, Melcher AH, Brunette DM (1977). Location of progenitor cells in periodontal ligament of mouse molar stimulated by wounding. *Anat Rec* 188:133-141.

Grzesik WJ, Kuznetsov SA, Uzawa K, Mankani M, Gehron Robey P, Yamauchi M (1998). Normal human cementum-derived cells: isolation, clonal expansion, and *in vitro* and *in vivo* characterization. *J Bone Miner Res* 13:1547-1554.

Hayashi Y (1985). Ultrastructural characterization of extracellular matrix vesicles in the mineralizing fronts of apical cementum in cats. *Arch Oral Biol* 30:445-449.

Hayashi Y (1989). Ultrastructural demonstration of the carbohydrate in developing rat enamel using soybean agglutinin-gold complexes. *Arch Oral Biol* 34:517-522.

Hayashi Y, Bianco P, Shimokawa H, Termine JD, Bonucci E (1986). Organic-inorganic relationships, and immunohistochemical localization of amelogenins and enamelins in developing enamel. *Basic Appl Histochem* 30:291-299.

Hayashi Y, Imai M, Goto Y, Murakami N (1993). Pathological mineralization in a serially passaged cell line from rat pulp. *J Oral Pathol Med* 22:175-179.

JCPDS (1998). Joint Committee on Powder Diffraction Standards No. 9-432 file for calcium hydroxyapatite.

Landis WJ, Paine MC, Glimcher MJ (1980). Use of acrolein vapors for the anhydrous preparation of bone tissue for electron microscopy. *J Ultrastruct Res* 70:171-180.

LeGeros RZ, Kojkowska R (1989). Synergistic effect of magnesium and carbonate on some properties of apatites (abstract). *J Dent Res* 68(Spec Iss):1003.

Lehninger AL (1970). Mitochondria and calcium ion transport. *Biochem J* 119:129-138.

MacNeil RL, D'Errico JA, Ouyang H, Berry J, Strayhorn C, Somerman MJ (1998). Isolation of murine cementoblasts: unique cells or uniquely-positioned osteoblasts? *Eur J Oral Sci* 106(Suppl I):350-356.

Matthews JL, Martin JH, Sampson HW, Kunin AS, Roan JH (1970). Mitochondrial granules in the normal and rachitic rat epiphysis. *Calcif Tissue Res* 5:91-99.

McCulloch CA, Melcher AH (1983). Cell migration in the periodontal ligament of mice. *J Periodont Res* 18:339-352.

McCulloch CA, Nemeth E, Lowenberg B, Melcher AH (1987). Paravascular cells in endosteal spaces of the alveolar bone contribute to periodontal ligament cell populations. *Anat Rec* 219:233-242.

Melcher AH, McCulloch CA, Cheong T, Nemeth E, Shiga A (1987). Cells from bone synthesize cementum-like and bone-like tissue *in vitro* and may migrate into periodontal ligament *in vivo*. *J Periodont Res* 22:246-247.

Narayanan AS, Page RC (1976). Biochemical characterization of collagens synthesized by fibroblasts derived from normal and diseased human gingiva. *J Biol Chem* 251:5464-5471.

Sasagawa I (1988). The appearance of matrix vesicles and mineralization during tooth development in three teleost fishes with well-developed enameloid and orthodentine. *Arch Oral Biol* 33:75-86.

Van Dijk K, Schaeken HG, Marée CHM, *et al.* (1995). Influence of Ar pressure on r.f. magnetron-sputtered $Ca_5(PO_4)_3OH$ layers. *Surf Coat Technol* 76:206-210.

Volpe P, Krause KH, Hashimoto S, Zorzato F, Pozzan T, Meldolesi J, *et al.* (1988). "Calciosome," a cytoplasmic organelle: the inositol 1,4,5-trisphosphate-sensitive Ca^{2+} store of nonmuscle cells? *Proc Natl Acad Sci USA* 85:1091-1095.

Wuthier RF (1982). A review of the primary mechanism of endochondral calcification with special emphasis on the role of cells, mitochondria and matrix vesicles. *Clin Orthop* 169:219-242.

Yamamoto T, Domon T, Takahashi S, Islam NM, Suzuki R, Wakita M (1998). The regulation of fiber arrangement in advanced cellular cementogenesis of human teeth. *J Periodont Res* 33:83-90.

Zimmermann B (1994). Occurrence of osteoblast necroses during ossification of long bone cortices in mouse fetuses. *Cell Tissue Res* 275:345-353.

Zimmermann B, Wachtel HC, Noppe C (1991). Patterns of mineralization *in vitro*. *Cell Tissue Res* 263:483-493.